

Long-term administration of scopolamine interferes with nerve cell proliferation, differentiation and migration in adult mouse hippocampal dentate gyrus, but it does not induce cell death

Bing Chun Yan¹, Joon Ha Park², Bai Hui Chen³, Jeong-Hwi Cho², In Hye Kim², Ji Hyeon Ahn², Jae-Chul Lee², In Koo Hwang⁴, Jun Hwi Cho⁵, Yun Lyul Lee³, Il-Jun Kang⁶, Moo-Ho Won²

1 Department of Integrative Traditional & Western Medicine, Medical College, Yangzhou University, Yangzhou, Jiangsu Province, China

2 Department of Neurobiology, School of Medicine, Kangwon National University, Chuncheon, South Korea

3 Department of Physiology, College of Medicine, Institute of Neurodegeneration and Neuroregeneration, Hallym University, Chuncheon, South Korea

4 Department of Anatomy and Cell Biology, College of Veterinary Medicine, Seoul National University, Seoul, South Korea

5 Department of Emergency Medicine, School of Medicine, Kangwon National University, Chuncheon, South Korea

6 Department of Food Science and Nutrition, Hallym University, Chuncheon, South Korea

Abstract

Bing Chun Yan and Joon Ha Park contributed equally to this article.

Corresponding author:

Moo-Ho Won, D.V.M., Ph.D.,

Department of Neurobiology, School of Medicine, Kangwon National University, Chuncheon 200-701, South Korea, mhwon@kangwon.ac.kr.

Il-Jun Kang, Ph.D., Department of Food Science and Nutrition, Hallym University, Chuncheon 200-702, South Korea, ijkang@hallym.ac.kr.

doi:10.4103/1673-5374.143415

http://www.nrronline.org/

Accepted: 2014-09-04

Long-term administration of scopolamine, a muscarinic receptor antagonist, can inhibit the survival of newly generated cells, but its effect on the proliferation, differentiation and migration of nerve cells in the adult mouse hippocampal dentate gyrus remain poorly understood. In this study, we used immunohistochemistry and western blot methods to weekly detect the biological behaviors of nerve cells in the hippocampal dentate gyrus of adult mice that received intraperitoneal administration of scopolamine for 4 weeks. Expression of neuronal nuclear antigen (NeuN; a neuronal marker) and Fluoro-Jade B (a marker for the localization of neuronal degeneration) was also detected. After scopolamine treatment, mouse hippocampal neurons did not die, and Ki-67 (a marker for proliferating cells)-immunoreactive cells were reduced in number and reached the lowest level at 4 weeks. Doublecortin (DCX; a marker for newly generated neurons)-immunoreactive cells were gradually shortened in length and reduced in number with time. After scopolamine treatment for 4 weeks, nearly all of the 5-bromo-2'-deoxyuridine (BrdU)-labeled newly generated cells were located in the subgranular zone of the dentate gyrus, but they did not migrate into the granule cell layer. Few mature BrdU/NeuN double-labeled cells were seen in the subgranular zone of the dentate gyrus. These findings suggest that long-term administration of scopolamine interferes with the proliferation, differentiation and migration of nerve cells in the adult mouse hippocampal dentate gyrus, but it does not induce cell death.

Key Words: nerve regeneration; neurogenesis; scopolamine; dentate gyrus; cell proliferation; neuroblast differentiation; neuroblast migration; granule cell layer; neural regeneration

Funding: This study was supported by the National Research Foundation of Korea (NRF) funded by the Ministry of Education, Science and Technology, No. 2010-0010580, and by Basic Science Research Program through the National Research Foundation of Korea (NRF) funded by the Ministry of Science, ICT and future Planning, No. NRF-2013R1A2A2A01068190.

Yan BC, Park JH, Chen BH, Cho JH, Kim IH, Ahn JH, Lee JC, Hwang IK, Cho JH, Lee YL, Kang IJ, Won MH. Long-term administration of scopolamine interferes with nerve cell proliferation, differentiation and migration in adult mouse hippocampal dentate gyrus, but it does not induce cell death. *Neural Regen Res.* 2014;9(19):1731-1739.

Introduction

The hippocampus of the mammalian brain is involved in cognitive processes such as learning and memory (Chen et al., 2012; Velazquez et al., 2013). Especially, the hippocampus is well known as a very sensitive region to physiological and pathological stimuli and shows structural and functional changes after various stimuli (Yan et al., 2012). Previous studies have shown that the structure of the mammalian hippocampus continues to be modified throughout the life by continuous addition of neurons in the dentate gyrus (DG;

Arabpoor et al., 2012; Pan et al., 2013; Zhang et al., 2013, 2014). Newly generated cells in the DG are mainly located in the subgranular zone of the DG, and they can migrate into the granule cell layer of the DG, in which they mature into new neurons and make functional synaptic connections for the hippocampal circuitry (Tanapat et al., 1999; Gage, 2000; Dayer et al., 2003). During the course of adult hippocampal neurogenesis, the postmitotic maturation and survival phase are closely associated with dendrite maturation (Plumpe et al., 2006; Ramirez-Rodriguez et al., 2011).

Scopolamine (SCO), a nonselective muscarinic receptor antagonist, is well known to interfere with the processes of learning acquisition and short-term memory in animals and humans (Jeong et al., 2008; Marisco et al., 2013). It has been well known that SCO impairs memory performance in both humans and animals (Grasby et al., 1995). It has been reported that SCO significantly increases acetylcholinesterase (AChE) and malondialdehyde (MDA) levels in the cortex and hippocampus (Shi et al., 2010; Tota et al., 2012a, b). Especially, SCO attenuates memory-task-induced increases of regional cerebral blood flow in the prefrontal cortex and the right anterior cingulate region (Grasby et al., 1995).

There are studies showing that subcutaneous administration of SCO *via* an Alzet osmotic pump for 4 weeks could significantly decrease the cell proliferation and neuroblast differentiation in the brain of rats (Yoo et al., 2011a, 2012). However, to the best of our knowledge, there have been no reports on neuroblast injury in the dentate gyrus after long-term administration of SCO. Therefore, in the present study, we examined chronological changes in the mutation and complexity of neuroblasts and their dendrite remodeling and maturation in the DG after long-term administration of SCO in mice.

Materials and Methods

Experimental animals

Adult male ICR mice, weighing 25–30 g, aged 8 weeks were purchased from Orient Bio Inc. (Seongnam, South Korea). These mice were housed at $23 \pm 3^\circ\text{C}$ and $55 \pm 5\%$ relative humidity in a 12-hour light/dark cycle and were allowed free access to food and water. The procedures for animal handling and care were in compliance with the current international laws and policies (Guide for the Care and Use of Laboratory Animals, the National Academies Press, 8th Ed., 2011), and they were approved by the Institutional Animal Care and Use Committee (IACUC) at Kangwon National University, South Korea. All efforts were also made to minimize animal suffering and the number of the animals used.

Administration of SCO and 5-bromo-2'-deoxyuridine (BrdU)

Mice in the SCO-treated groups were intraperitoneally injected with 1 mg/kg of SCO (Sigma S1875, Bangalore, product of India), once daily, for 1–4 weeks ($n = 14$ at each time point). The control mice ($n = 14$ at each time point) were injected with the same volume of saline (pH 7.4). Doses of SCO were selected based on previous studies (Wang et al., 2013; Heo et al., 2014a, b). The mice were then sacrificed after 1-, 2-, 3- and 4-week treatment. In addition, to label the mitotic cells in the DG, control and 4 weeks-SCO-treated mice were intraperitoneally injected with 50 mg/kg BrdU (Sigma, St. Louis, MO, USA) for twice at a 8 hour interval on days 6, 13, 20 and 27 during the experiment according to previous studies (Lee et al., 2012; Chen et al., 2013).

Tissue processing for histology

For histological analysis, mice were anesthetized by intra-

peritoneal injection of sodium pentobarbital and perfused transcardially with 0.1 mol/L PBS (pH 7.4) followed by 4% paraformaldehyde in 0.1 mol/L phosphate buffer (pH 7.4). Their brains were removed and postfixed by 4% paraformaldehyde in 0.1 mol/L phosphate-buffer (pH 7.4) for 4 hours at 4°C . The brain tissues were cryoprotected by infiltration with 30% sucrose overnight. Thereafter, frozen tissues were serially sectioned on a cryostat (Leica, Wetzlar, Germany) into 30- μm thick coronal sections. To get satisfactory immunolabeling results and to avoid the side effect of paraformaldehyde fixation, free floating sections were selected for immunohistochemical staining and then transferred into 6-well plates containing PBS.

Immunohistochemistry for NeuN, BrdU, Ki-67 and DCX

To obtain the accurate data for immunohistochemistry, 15 sections per mouse were selected from the control- and SCO-treated group under the same conditions. For BrdU immunostaining, DNA denaturation was conducted and the sections were incubated in 2 mol/L HCl and in boric acid. The sections were sequentially treated with 0.3% hydrogen peroxide (H_2O_2) in PBS for 30 minutes and incubated in 10% normal goat serum in 0.05 mol/L PBS or Mouse-On-Mouse (M.O.M.) mouse Ig blocking reagent to get rid of the background staining due to the presence of endogenous mouse Ig (diluted at 1:10; Vector, Burlingame, CA, USA) for 30 minutes. They were diluted into mouse anti-NeuN (a neuronal marker; 1:1000; Chemicon, Temecula, CA, USA, MAB 377), mouse anti-BrdU (1:250; BioSource International, Camarillo, CA, USA), rabbit anti-Ki-67 (a marker for cell proliferation; 1:100; Abcam, Cambridge, UK) and goat anti-doublecortin (DCX; a marker for neuroblasts; 1:200; Santa Cruz Biotechnology, Santa Cruz, CA, USA) antibody overnight at 4°C and subsequently exposed to M.O.M. biotinylated anti-mouse IgG or biotinylated goat anti-rabbit and rabbit anti-goat IgG for 2 hours at room temperature and streptavidin peroxidase complex (diluted at 1:200; Vector, Burlingame) for 1 hour at room temperature. They were then visualized by reacting to 3,3'-diaminobenzidine tetrachloride (Sigma) in 0.1 mol/L Tris-HCl buffer (pH 7.2) and mounted on gelatin-coated slides. After dehydration, the sections were mounted in canada balsam (Kanto Chemical, Tokyo, Japan).

Fifteen sections per mouse were selected to quantitatively analyze DCX immunoreactivity and determine the number of NeuN-, BrdU-, Ki-67- and DCX-immunoreactive cells. DCX immunoreactivity and the number of NeuN-, BrdU-, Ki-67- and DCX-immunoreactive cells in all the groups were determined using a BX51 light microscope (Olympus, Tokyo, Japan) equipped with a digital camera (DP71, Olympus) connected to a PC monitor. The dendritic complexity of the DCX-immunoreactive neuroblasts was traced using a camera lucida at $100 \times$ and $400 \times$ magnification (Neurolucida; MicroBrightField, Williston, VT, USA). The DCX-immunoreactive cells were separated into three types according to dendritic complexity. The first type contained cells that lacked dendrites or had shorter dendrites than the soma size.

The secondary type contained cells that had one primary dendrite with one branch. The third type contained cells that had much branches reaching the molecular layer. Cell counts for DCX (including three types), Ki-67-immunoreactive and BrdU-positive cells were presented as the mean number of the cells per section. For relative analysis as percent values in types of DCX-immunoreactive cells, a ratio of three types in the total number of DCX-immunoreactive cells was calibrated as %, with all groups designated as 100%. The cell counts for NeuN-positive cells were represented as the number in 1 mm^2 in the granule cell layer of the DG.

In order to quantitatively analyze the DCX immunoreactivity, the images were digitized into an array of 512×512 pixels corresponding to a tissue area of $140 \times 140 \mu\text{m}^2$ ($40 \times$ primary magnification). Each pixel resolution was 256 gray levels. The DCX-immunoreactive cell structures were evaluated on the basis of an optical density (OD), which was obtained after the transformation of the mean gray level using the formula: $\text{OD} = \log(256/\text{mean gray level})$. The OD of background was taken from areas adjacent to the measured area. After subtracting the OD of background, a ratio of the OD of image file was calibrated as % (relative OD, ROD) using Adobe Photoshop version 8.0 and then analyzed using NIH Image 1.59 software. A ratio of the ROD was calibrated as %, with control group designated as 100 %.

Fluoro-Jade B histofluorescence

To examine the neuronal death in the hippocampus after SCO treatment, the sections ($n = 7$ per mouse) were stained by Fluoro-Jade B (F-J B, a high affinity fluorescent marker for the localization of neuronal degeneration) histofluorescence under the same conditions. F-J B histofluorescence staining procedures were conducted according to the method as previously described (Candelario-Jalil et al., 2003; Yu et al., 2012). In brief, the sections were first immersed in a solution containing 1% sodium hydroxide in 80% alcohol, and then in 70% alcohol. They were then transferred to a solution of 0.06% potassium permanganate, followed by a 0.0004% F-J B (Histochem, Jefferson, AR, USA) staining solution. After washing, the sections were placed on a slide warmer (approximately 50°C) for examination using an epifluorescent microscope (Carl Zeiss, Germany) with blue (450–490 nm) excitation light and a barrier filter. With this method, neurons that undergo degeneration brightly fluoresce in comparison to the background (Schmued and Hopkins, 2000). As a positive control, we added a finding using histofluorescence procedure in the hippocampal DG damaged by transient cerebral ischemia.

Double immunofluorescence

To confirm the differentiation from newly generated cells into mature neurons, double immunofluorescence staining for BrdU and NeuN was performed. DNA denaturation was conducted with below mentioned protocol. For BrdU immunostaining to visualize BrdU-labeled nuclei: 2 hour incubation in 50% formamide/ $2 \times$ SSC (0.3 mol/L NaCl, 0.03 mol/L sodium citrate) at 65°C , 30-minute incubation in 2 N HCl at

37°C , and 10-minute rinse in 0.1 mol/L boric acid (pH 8.5). After this, the sections were incubated in the mixture of rat anti-BrdU (1:100; BioSource International, Camarillo, CA, USA) and rabbit anti-NeuN (1:500; Chemicon International Inc., Temecular, CA, USA) overnight at 4°C . They were then incubated in a mixture of both FITC-conjugated anti-rat IgG (1:200; Jackson ImmunoResearch, West Grove, PA, USA) and Cy3-conjugated anti-rabbit IgG (1:500; Jackson ImmunoResearch) for 2 hours at room temperature. The immunoreactions were observed under the confocal MS (LSM510 META NLO, Carl Zeiss). FITC was detected within a range of 500–550 nm following fluorophore excitation by 488 nm Ar-laser. For Cy3, detection was in 570–630 range following excitation by the 561 nm HeNe laser. Cell counts were performed following the above-mentioned method.

Western blot analysis

To obtain the accurate data for change in DCX protein level in the hippocampus after SCO treatment, the control and SCO-treated mice ($n = 7$ at each time point) were used for western blot analysis. After sacrifice, the brain tissue was serially and transversely cut into a thickness of 400 μm on a vibratome (Leica), and the hippocampal region was then dissected with a surgical blade. The tissues were homogenized in 50 mmol/L PBS (pH 7.4) containing 0.1 mmol/L ethylene glycol-bis(2-aminoethyl Ether)-N,N,N',N'-tetraacetic acid (EGTA) (pH 8.0), 0.2% Nonidet P-40, 10 mmol/L ethylenediamine tetraacetic acid (EDTA) (pH 8.0), 15 mmol/L sodium pyrophosphate, 100 mmol/L β -glycerophosphate, 50 mmol/L NaF, 150 mmol/L NaCl, 2 mmol/L sodium orthovanadate, 1 mmol/L phenylmethylsulfonyl fluoride (PMSF) and 1 mmol/L dithiothreitol (DTT). After centrifugation, the protein level in the supernatants was determined using a micro BCA protein assay kit with bovine serum albumin as a standard (Pierce Chemical, Rockford, IL, USA). Aliquots containing 50 μg of total protein were boiled in loading buffer containing 150 mmol/L Tris (pH 6.8), 3 mmol/L DTT, 6% SDS, 0.3% bromophenol blue and 30% glycerol. The aliquots were then loaded onto a 5% polyacrylamide gel. After electrophoresis, the gels were transferred to nitrocellulose membranes (Pall Crop, East Hills, NY, USA). To reduce background staining, the membranes were incubated with 5% non-fat dry milk in PBS containing 0.1% Tween 20 for 45 minutes, followed by incubation with goat antibody antiserum (1:200), peroxidase-conjugated rabbit anti-goat IgG (Sigma) and an ECL kit (Pierce Chemical). The result of western blot analysis was scanned, and densitometric analysis for the quantification of the bands was done using Scion Image software (Scion Corp., Frederick, MD, USA), which was used to count relative optical density (ROD): A ratio of the ROD was calibrated as %, with sham group designated as 100 %.

Data analysis

Data are expressed as the mean \pm SEM. Data from NeuN, Ki-67 and DCX immunohistochemistry and DCX western blot analysis were analyzed by one-way analysis of variance followed by a Tukey's multiple range method in order to

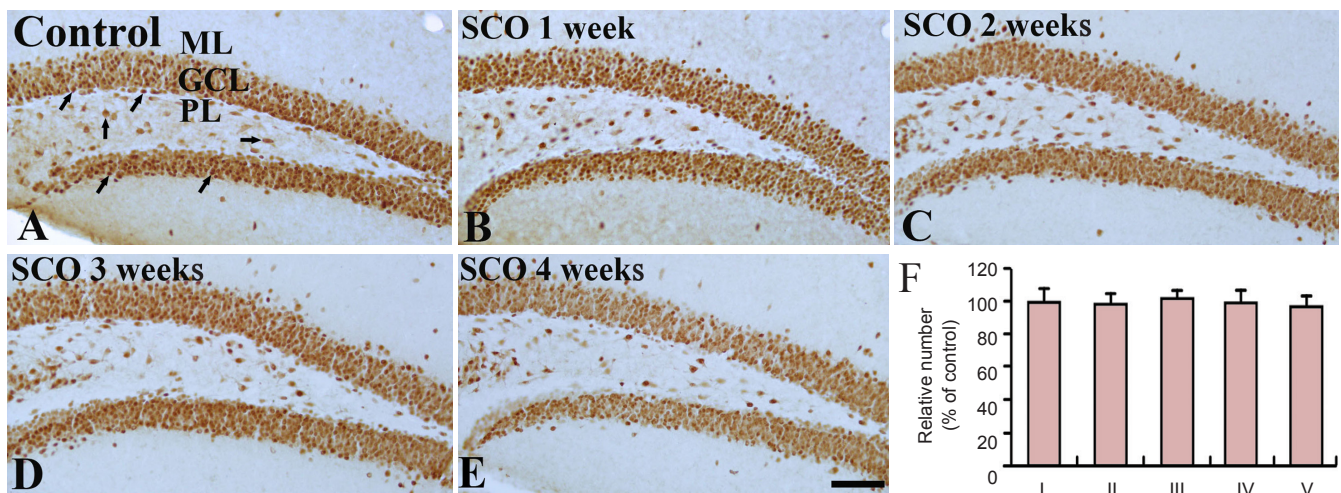


Figure 1 NeuN immunohistochemistry in the dentate gyrus of the control and SCO-treated (1–4 weeks) groups. In the control group (A), NeuN-positive cells (arrows) are well detected in the hippocampal dentate gyrus. NeuN-positive cells in all the SCO-treated (1–4 weeks) groups (B–E) are similar to those in the control group. Scale bar: 200 μ m. (F) The percent of the number of NeuN-positive cells/mm² in the GCL of the hippocampal dentate gyrus. Data were analyzed using one-way analysis of variance followed by a Tukey’s multiple range method ($n = 7$ per group). The bars indicate the mean \pm SEM. SCO: Scopolamine; GCL: granule cell layer; ML: molecular layer; PL: polymorphic layer; I: control; II: SCO 1 week; III: SCO 2 weeks; IV: SCO 3 weeks; V: SCO 4 weeks.

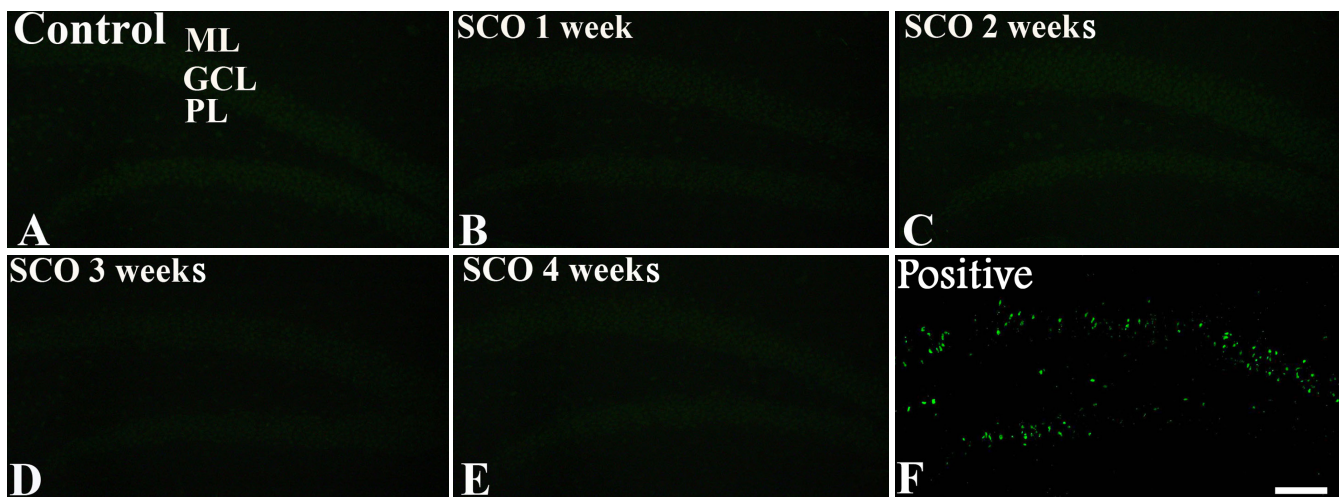


Figure 2 Fluoro-Jade B histofluorescence staining in the dentate gyrus of the control and SCO-treated (1–4 weeks) groups. Fluoro-Jade B positive cells (green) are hardly detected in the control (A) and SCO-treated (1–4 weeks) groups (B–E). (F) Positive control shows Fluoro-Jade B positive cells in the dentate gyrus. SCO: Scopolamine; ML: molecular layer; GCL: granule cell layer; PL: polymorphic layer. Scale bar: 200 μ m.

elucidate differences among experimental groups. Data from BrdU immunohistochemistry and BrdU/NeuN double immunofluorescence staining were analyzed by independent samples *t*-tests in order to elucidate differences between the control and 4 weeks-SCO-treated groups. Statistical significance was considered at $P < 0.05$.

Results

Neuronal damage

Neuronal damage in the hippocampal DG after SCO treatment was examined by NeuN immunohistochemistry and F-J B histofluorescence staining. NeuN-positive cells were easily observed in the hippocampal DG of the control group (Figure 1A, F), and, in all of SCO-treated groups, the distribution of NeuN-positive cells was not different from that in

the control group (Figure 1B–F). Neuronal degeneration in the hippocampal DG after SCO treatment was examined by F-J B histofluorescence staining (Figure 2B–E). F-J B-positive cells were not observed in the hippocampal DG of all the experimental groups.

Changes in cell proliferation and neuroblast differentiation

Cell proliferation

Ki-67-immunoreactive cells were mainly detected in the subgranular zone of the hippocampal DG (Figure 3). In the control group, many Ki-67-immunoreactive cells in the DG were observed (Figure 3A). After 1 and 2 weeks of SCO treatment, the number of Ki-67-immunoreactive cells was slightly decreased compared with that in the control group

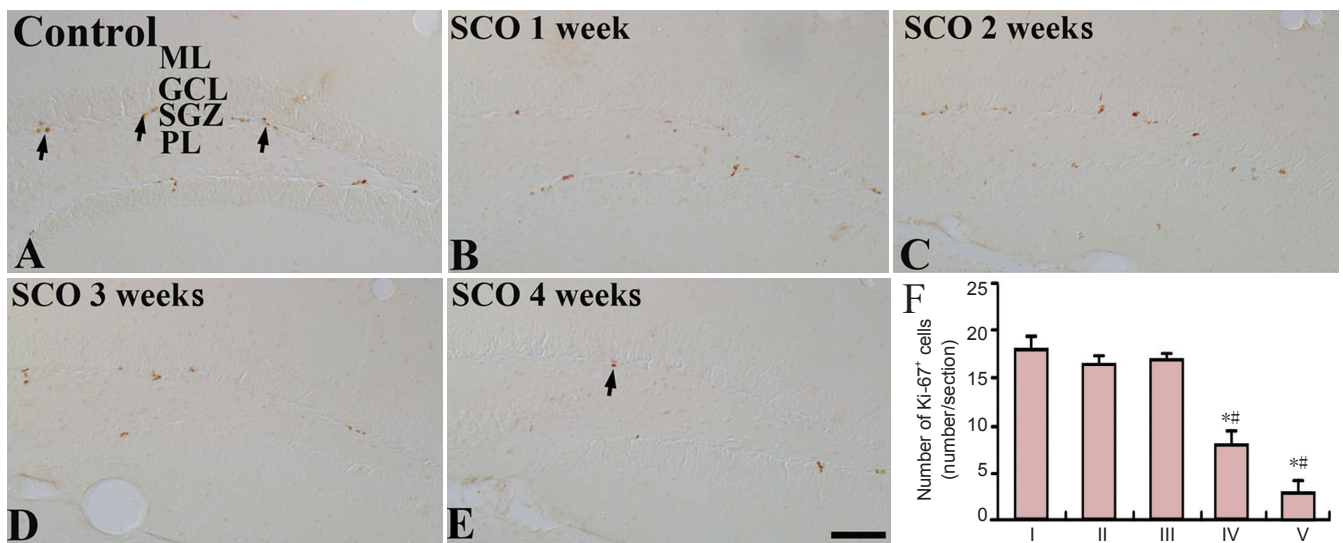


Figure 3 Ki-67 immunohistochemistry in the dentate gyrus of the control and SCO-treated (1–4 weeks) groups. Ki-67-immunoreactive cells (arrows) in the 4 weeks-SCO-treated group (E) are much less than those in the control group (A). (B–D) 1–3 weeks-SCO-treated groups. Scale bar: 50 μ m. (F) Mean number of Ki-67-immunoreactive cells per section in the dentate gyrus. Data were analyzed using one-way analysis of variance followed by a Tukey’s multiple range method ($n = 7$ per group; $*P < 0.05$, vs. the control group; $\#P < 0.05$, vs. the former time point group). The bars indicate the mean \pm SEM. SCO: Scopolamine; ML: molecular layer; GCL: granule cell layer; SGZ: subgranular zone; PL: polymorphic layer; I: control; II: SCO 1 week; III: SCO 2 weeks; IV: SCO 3 weeks; V: SCO 4 weeks.

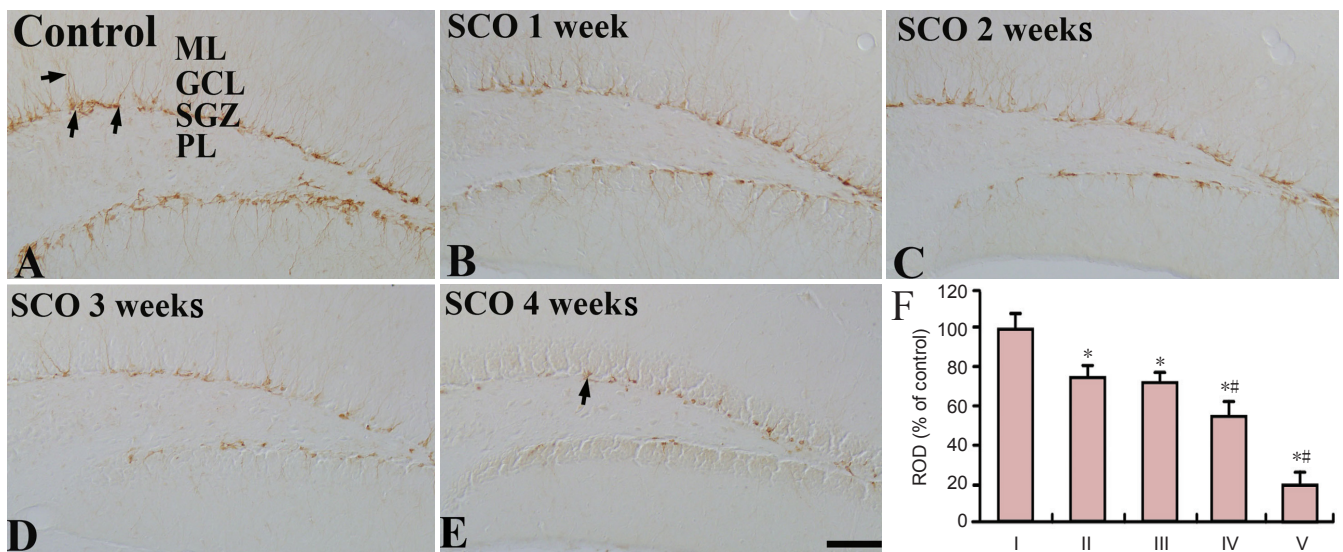


Figure 4 DCX immunohistochemistry in the subgranular zone of the dentate gyrus of the control and SCO-treated (1–4 weeks) groups. DCX-immunoreactive cells (arrows) in the 4 weeks-SCO-treated group (E) are much less than those in the control group (A). (B–D) 1–3 weeks-SCO-treated groups. Scale bar: 50 μ m. (F) Relative optical density of DCX immunoreactivity in the dentate gyrus. Data were analyzed using one-way analysis of variance followed by a Tukey’s multiple range method ($n = 7$ per group; $*P < 0.05$, vs. the control group; $\#P < 0.05$, vs. the former time point group). The bars indicate the mean \pm SEM. DCX: Doublecortin; SCO: scopolamine; ML: molecular layer; GCL: granule cell layer; SGZ: subgranular zone; PL: polymorphic layer; ROD: relative optical density; I: control; II: SCO 1 week; III: SCO 2 weeks; IV: SCO 3 weeks; V: SCO 4 weeks.

(Figure 3B, C). The mean number of Ki-67-immunoreactive cells after 3 weeks of SCO treatment was significantly decreased (about 40% of the control group) ($P < 0.05$; Figure 3D, F). After 4 weeks of SCO treatment, the mean percent of the mean number of Ki-67-immunoreactive cells was about 17% of the control group ($P < 0.05$; Figure 3E, F).

Neuroblast differentiation

DCX-immunoreactive cells were mainly detected in the subgranular zone of the DG in all the SCO-treated groups (Figure 4). In the control group, many DCX-immunoreac-

tive cells were observed in the subgranular zone (Figure 4A). At 1 and 2 weeks after SCO treatment, DCX immunoreactivity was significantly decreased compared to that in the control group ($P < 0.05$; Figure 4B, C and F), and, after 3 and 4 weeks of SCO treatment, DCX immunoreactivity was significantly decreased by about 50% and 80%, respectively, compared with that in the control group ($P < 0.05$; Figure 4D, E and F). Especially, many dendrites of DCX-immunoreactive cells were lost in the DG after 4 weeks of SCO treatment (Figure 4E). Also, changes in the mean number of DCX-immunoreactive cells were similar to the results of

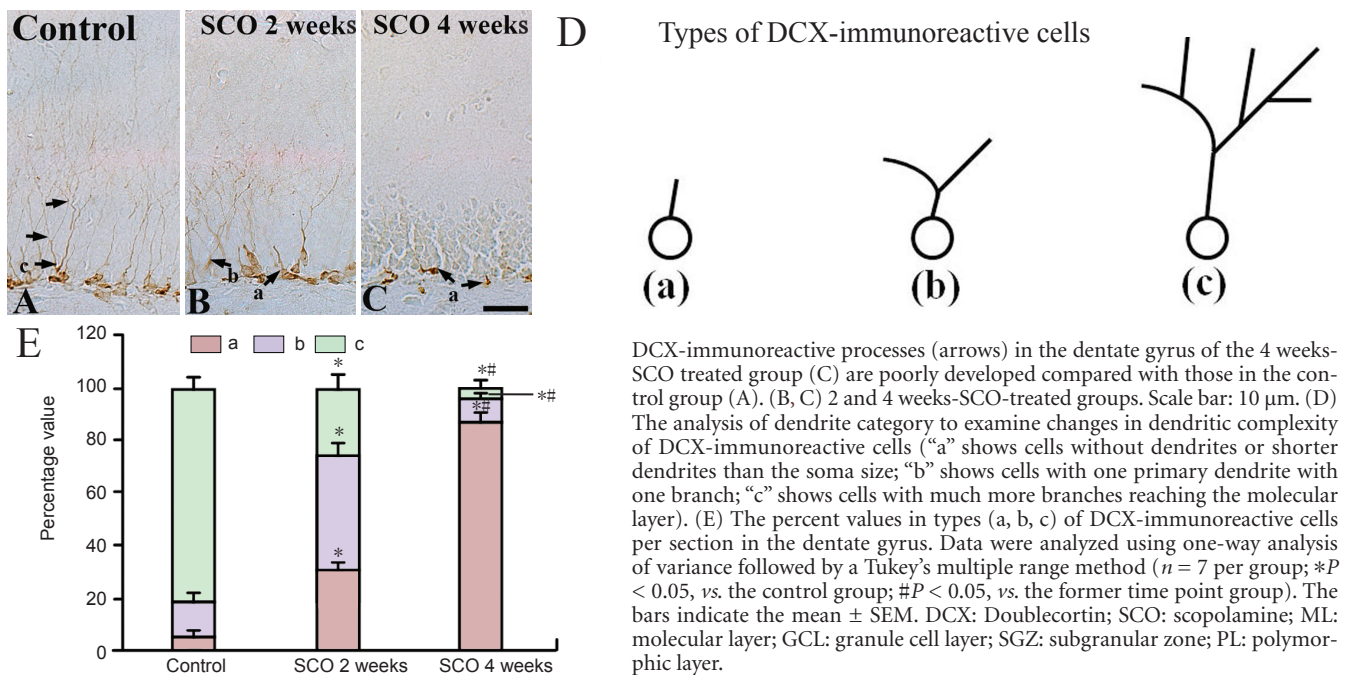


Figure 5 High magnification of DCX immunohistochemistry in the dentate gyrus of the control and SCO-treated (2 and 4 weeks) groups.

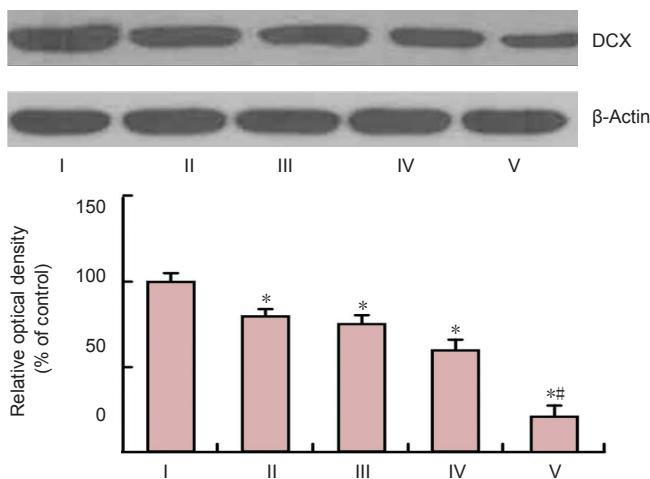


Figure 6 Western blot analysis of DCX in the dentate gyrus of the control and SCO-treated (1–4 weeks) groups.

Data were analyzed using one-way analysis of variance followed by a Tukey’s multiple range method ($n = 7$, $*P < 0.05$, vs. the control group, $\#P < 0.05$, vs. the former groups). The bars indicate the mean \pm SEM. ROD: Relative optical density; DCX: doublecortin; SCO: scopolamine; wk: week(s); I: control; II: SCO 1 week; III: SCO 2 weeks; IV: SCO 3 weeks; V: SCO 4 weeks.

DCX immunoreactivity (Table 1).

In addition, we classified DCX-immunoreactive dendrites into three types according to the previously described method (Chen et al., 2013). In the control group, most of DCX-immunoreactive cells had dendrites of type “c”: The dendrites were thickened and became very long, which projected into the molecular layer of the DG (Figure 1A). However, in the 2 weeks-SCO-treated group, many DCX-immunoreactive cells had dendrites of type “a” and “b”, and most of DCX-immunoreactive cells had dendrites of type “a” in

the 4 weeks-SCO-treated group (Figure 5B, C). (D) The analysis of dendrite category to examine changes in dendritic complexity of DCX-immunoreactive cells (“a” shows cells without dendrites or shorter dendrites than the soma size; “b” shows cells with one primary dendrite with one branch; “c” shows cells with much more branches reaching the molecular layer). (E) The percent values in types (a, b, c) of DCX-immunoreactive cells per section in the dentate gyrus. Data were analyzed using one-way analysis of variance followed by a Tukey’s multiple range method ($n = 7$ per group; $*P < 0.05$, vs. the control group; $\#P < 0.05$, vs. the former time point group). The bars indicate the mean \pm SEM. DCX: Doublecortin; SCO: scopolamine; ML: molecular layer; GCL: granule cell layer; SGZ: subgranular zone; PL: polymorphic layer.

Table 1 Changes in the mean number of DCX-immunoreactive cells per section in the hippocampal DG of the control and SCO-treated (1–4 weeks) groups

Group	Number of DCX-immunoreactive cells
Control	83 \pm 6.64
SCO 1 week	57 \pm 5.81*
SCO 2 weeks	51 \pm 2.35*
SCO 3 weeks	36 \pm 3.26**
SCO 4 weeks	21 \pm 2.92**

Data were analyzed by one-way analysis of variance followed by Tukey’s multiple range method ($n = 7$ per group). $*P < 0.05$, vs. the control group; $\#P < 0.05$, vs. the former group. DCX: Doublecortin; DG: dentate gyrus; SCO: scopolamine.

the 4 weeks-SCO-treated group (Figure 5B, C).

DCX protein level

Western blot analysis showed that the level of DCX protein was changed in the DG after SCO treatment (Figure 6). The protein level of DCX was significantly decreased after SCO treatment compared to that in the control group ($P < 0.05$), and after 4 weeks of SCO treatment, the mean percent of DCX protein level was about 19% of the control group (Figure 6).

Integration of newly generated cells into granule cells

The distribution of the BrdU-positive cells was observed in the control and 4 weeks-SCO-treated groups (Figure 7). In the control group, many BrdU-positive cells were found in the subgranular zone of the DG, and some BrdU-positive cells migrated into the granule cell layer (Figure 7A, a). After 4 weeks of SCO treatment, BrdU-positive cells were significantly decreased (about 22% of the control group) ($P < 0.05$),

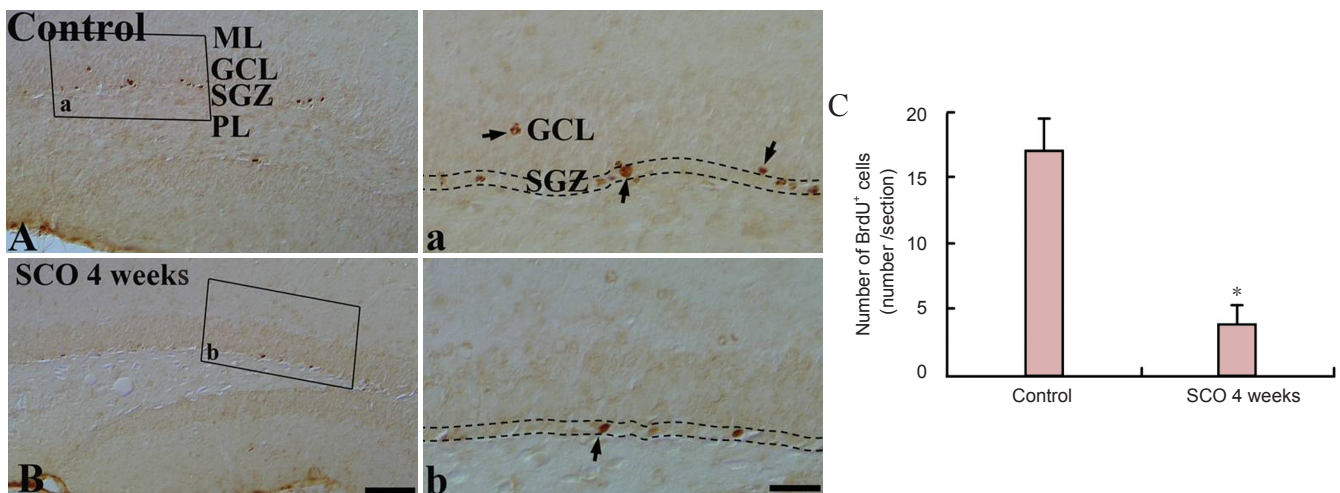


Figure 7 BrdU immunohistochemistry in the dentate gyrus of the control and 4 weeks-SCO-treated groups. The number of BrdU-positive cells (arrows) in the SGZ (indicated by dashed wavy lines) of the 4 weeks-SCO-treated group (B, b) is significantly decreased compared with that in the control group (A, a). Scale bars: 200 μ m for A, B, and 50 μ m for a and b. (C) The mean number of BrdU-positive cells per section in the dentate gyrus. Data were analyzed using an independent samples *t*-test ($n = 7$ per group; $*P < 0.05$, vs. the control group). The bars indicate the mean \pm SEM. BrdU: 5-Bromo-2'-deoxyuridine; SCO: scopolamine; ML: molecular layer; GCL: granule cell layer; SGZ: subgranular zone; PL: polymorphic layer.

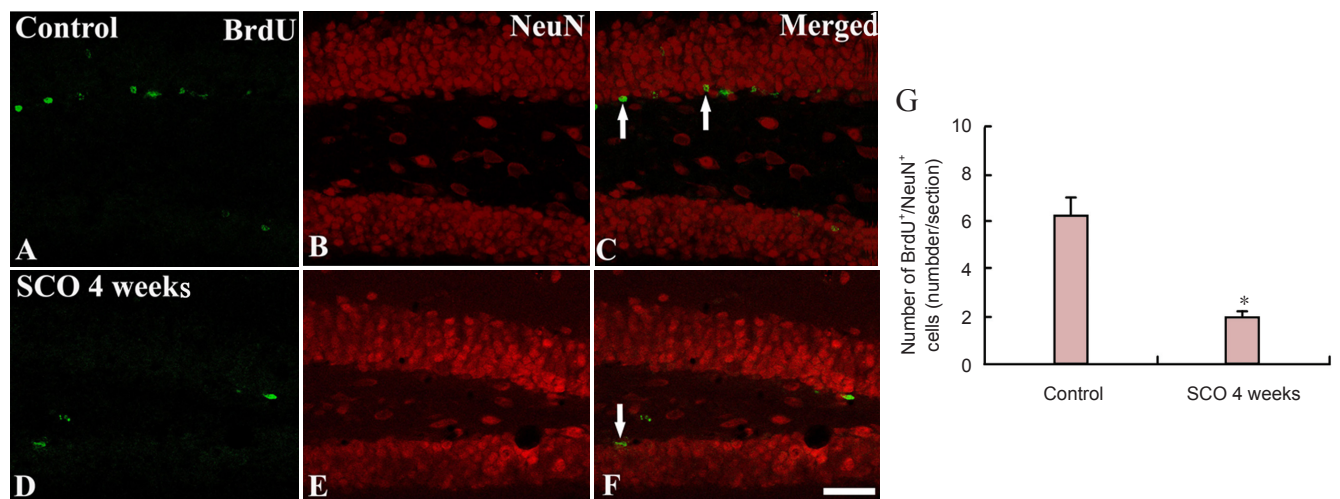


Figure 8 Confocal image of double-labeled cells with BrdU, NeuN, and merged images in the dentate gyrus of rats. Confocal image of double-labeled cells with BrdU (green; A, D) and NeuN (red; B, E) and merged image (C, F) in the control and 4 weeks-SCO-treated groups. Few BrdU/NeuN-immunoreactive cells (arrows) were found in the 4 weeks-SCO-treated group. Scale bar: 200 μ m. (G) The mean number of BrdU/NeuN-immunoreactive cells per section in the dentate gyrus. Data were analyzed using an independent samples *t*-test ($n = 7$ per group; $*P < 0.05$, vs. the control group). The bars indicate the mean \pm SEM. BrdU: 5-Bromo-2'-deoxyuridine; NeuN: neuronal nuclear antigen; SCO: scopolamine.

and no BrdU-positive cells were found in the granule cell layer (Figure 7B, b).

On the other hand, we carried out double staining for BrdU/NeuN to find new mature cells in the DG after SCO treatment, and we found that new mature cells, which showed the co-expression of BrdU/NeuN, were significantly decreased in numbers in the DG of mice in the 4 weeks-SCO-treated group than in the control group ($P < 0.05$; Figure 8).

Discussion

It has been reported that SCO could suppress the survival of newly generated cells in the mammalian brain and no mature neurons are damaged by SCO treatment (Kotani et al., 2006; Yoo et al., 2011b). Recently, Chen et al. (2014) showed

that SCO directly resulted in a damage of the hippocampal circuits that might predominantly be responsible for cognitive and memory deficits. It exhibited neurotoxicity on the population and dendritic development of newborn neurons and immature granular cells in the DG. Therefore, in the present study, we further examined the chronological effects of long term systemic SCO treatment on adult neurogenesis that concerns to dendrite maturation and complexity of neuronal progenitor cells. In addition, we, in the present study, first examined whether the neuronal damage/death occurred by NeuN immunohistochemistry and F-J B histo-fluorescence staining, and we did not observe any neuronal damage/death in the hippocampal DG following 4 weeks of SCO treatment. In the present study, we used intraperitone-

al injection instead of subcutaneous injection by an ALzet osmotic minipump, which was used in the above studies. In animals, intraperitoneal injection is predominantly used in veterinary medicine and animal testing for the systemic administration of drugs because it is an ease of administration compared with other parenteral methods (Park et al., 2012).

In the present study, we observed that the chronic systemic treatment with SCO induced change in cell proliferation in the mouse hippocampal DG. Ki-67, as a marker for endogenous proliferation, was used in this study to examine change in cell proliferation after SCO treatment. The numbers of Ki-67-positive cells was significantly decreased in the DG at 4 weeks after SCO treatment compared with the other groups.

In addition, we observed the morphological changes and proliferation of neuronal progenitor cells (neuroblasts) in the hippocampal DG after SCO treatment using DCX immunohistochemistry. Our finding showed that the arborization of DCX-immunoreactive processes in the DG was much worse and less in number than that in the control group at 4 weeks after SCO treatment. It has well been known that dendrite maturation in neuroblasts is associated with survival of newborn neurons (Plumpe et al., 2006). A previous report showed that change in dendrite complexity corresponded to synaptic connections of granular cells in the molecular layer of the DG (Ramirez-Rodriguez et al., 2011). We also found that the numbers of DCX-immunoreactive cells were significantly decreased in the DG at 4 weeks after SCO treatment compared with the control group. Therefore, our result indicates that chronic systemic treatment with SCO could impair the dendrite maturation and complexity of neuronal progenitor cells as well as the proliferation of neuronal progenitor cells and affect the synaptic function of them in the hippocampal DG.

On the other hand, it was reported that neural stem cells could generate both neurons and glial cells in some *in vitro* and *in vivo* experiments: the neural stem cells migrated into the granule cell layer and extended axonal fibers to the pyramidal cell layer of the hippocampal CA3 area within 4 to 10 days after mitosis (Palmer et al., 1999; Cameron and McKay, 2001), and, they become mature neurons expressing NeuN at about 4 weeks later (Ming and Song, 2005; Fujioka and Akema, 2010). In addition, Fujioka and Akema (2010) proved that the co-expression of BrdU-positive cells and NeuN-positive cells was found in the subgranular zone and granule cell layer of the rat DG 28 days after BrdU labeling. In the present study, we examined whether the chronic systemic treatment with SCO disrupted cell maturation in the mouse hippocampal DG using BrdU, as a marker for exogenous proliferation. The number of BrdU-positive cells was also significantly decreased in the DG at 4 weeks after SCO treatment compared with that in the other groups. In addition, we found that long-term treatment with SCO significantly reduced BrdU/NeuN co-expression in the mouse DG. This finding indicates that the ability of neuronal progenitor cell migration and differentiation is destroyed by SCO, and we suggest that the long-term treatment of SCO disrupts

neuroblasts to become mature neurons in the granule cell layer of the DG.

In conclusion, our results showed that chronic systemic treatment with SCO significantly disrupted cell proliferation, differentiation and maturation, especially, impaired the dendrite maturation and complexity of neuronal progenitor cells in the mouse hippocampal DG. Based on these findings, we suggest that an impairment of neurogenesis in the hippocampal DG could occur by SCO treatment and that SCO interferes with adult neurogenesis and is beneficial for studies to investigate the injury/recovery of neuronal progenitor cells' function in the brain.

Acknowledgements: We would like to thank Mr. Lee SU from the Kangwon National University, South Korea for his technical help in taking confocal microscope images in this study.

Author contributions: Yan BC drafted the manuscript. All authors participated in the design, implementation and evaluation of this study and approved the final version of this paper.

Conflicts of interest: None declared.

References

- Arabpoor Z, Hamidi G, Rashidi B, Shabrang M, Alaei H, Sharifi MR, Salami M, Dolatabadi HR, Reisi P (2012) Erythropoietin improves neuronal proliferation in dentate gyrus of hippocampal formation in an animal model of Alzheimer's disease. *Adv Biomed Res* 1:50.
- Cameron HA, McKay RD (2001) Adult neurogenesis produces a large pool of new granule cells in the dentate gyrus. *J Comp Neurol* 435:406-417.
- Candelario-Jalil E, Alvarez D, Merino N, Leon OS (2003) Delayed treatment with nimesulide reduces measures of oxidative stress following global ischemic brain injury in gerbils. *Neurosci Res* 47:245-253.
- Chen BH, Yan BC, Park JH, Ahn JH, Lee DH, Kim IH, Cho JH, Lee JC, Kim SK, Lee B, Won MH, Lee YL (2013) Aripiprazole, an atypical antipsychotic drug, improves maturation and complexity of neuroblast dendrites in the mouse dentate gyrus via increasing superoxide dismutases. *Neurochem Res* 38:1980-1988.
- Chen W, Cheng X, Chen J, Yi X, Nie D, Sun X, Qin J, Tian M, Jin G, Zhang X (2014) Lycium barbarum polysaccharides prevent memory and neurogenesis impairments in scopolamine-treated rats. *PLoS One* 9:e88076.
- Chen Y, Wang Z, Xie Y, Guo X, Tang X, Wang S, Yang S, Chen K, Niu Y, Ji W (2012) Folic acid deficiency inhibits neural rosette formation and neuronal differentiation from rhesus monkey embryonic stem cells. *J Neurosci Res* 90:1382-1391.
- Dayer AG, Ford AA, Cleaver KM, Yassae M, Cameron HA (2003) Short-term and long-term survival of new neurons in the rat dentate gyrus. *J Comp Neurol* 460:563-572.
- Fujioka H, Akema T (2010) Lipopolysaccharide acutely inhibits proliferation of neural precursor cells in the dentate gyrus in adult rats. *Brain Res* 1352:35-42.
- Gage FH (2000) Mammalian neural stem cells. *Science* 287:1433-1438.
- Grasby PM, Frith CD, Paulesu E, Friston KJ, Frackowiak RS, Dolan RJ (1995) The effect of the muscarinic antagonist scopolamine on regional cerebral blood flow during the performance of a memory task. *Exp Brain Res* 104:337-348.
- Heo YM, Shin MS, Kim SH, Kim TW, Baek SB, Baek SS (2014a) Treadmill exercise ameliorates disturbance of spatial learning ability in scopolamine-induced amnesia rats. *J Exerc Rehabil* 10:155-161.
- Heo YM, Shin MS, Lee JM, Kim CJ, Baek SB, Kim KH, Baek SS (2014b) Treadmill exercise ameliorates short-term memory disturbance in scopolamine-induced amnesia rats. *Int Neurol J* 18:16-22.
- Jeong EJ, Lee KY, Kim SH, Sung SH, Kim YC (2008) Cognitive-enhancing and antioxidant activities of iridoid glycosides from *Scrophularia buergeriana* in scopolamine-treated mice. *Eur J Pharmacol* 588:78-84.

- Kotani S, Yamauchi T, Teramoto T, Ogura H (2006) Pharmacological evidence of cholinergic involvement in adult hippocampal neurogenesis in rats. *Neuroscience* 142:505-514.
- Lee TH, Lee CH, Kim IH, Yan BC, Park JH, Kwon SH, Park OK, Ahn JH, Cho JH, Won MH, Kim SK (2012) Effects of ADHD therapeutic agents, methylphenidate and atomoxetine, on hippocampal neurogenesis in the adolescent mouse dentate gyrus. *Neurosci Lett* 524:84-88.
- Marisco PC, Carvalho FB, Rosa MM, Girardi BA, Gutierrez JM, Jaques JA, Salla AP, Pimentel VC, Schetinger MR, Leal DB, Mello CF, Rubim MA (2013) Piracetam prevents scopolamine-induced memory impairment and decrease of NTPDase, 5'-nucleotidase and adenosine deaminase activities. *Neurochem Res* 38:1704-1714.
- Ming GL, Song H (2005) Adult neurogenesis in the mammalian central nervous system. *Annu Rev Neurosci* 28:223-250.
- Palmer TD, Markakis EA, Willhoite AR, Safar F, Gage FH (1999) Fibroblast growth factor-2 activates a latent neurogenic program in neural stem cells from diverse regions of the adult CNS. *J Neurosci* 19:8487-8497.
- Pan YW, Wang W, Xia Z (2013) Assessment of adult neurogenesis in mice. *Curr Protoc Toxicol* Chapter 12:Unit12 20.
- Park SM, Yan BC, Park JH, Choi JH, Yoo KY, Lee CH, Baek YY, Kim YM, Kang IJ, Won MH (2012) Gliosis in the mice hippocampus without neuronal death after systemic administration of high dosage of tetanus toxin. *Cell Mol Neurobiol* 32:423-434.
- Plumpe T, Ehninger D, Steiner B, Klempin F, Jessberger S, Brandt M, Romer B, Rodriguez GR, Kronenberg G, Kempermann G (2006) Variability of doublecortin-associated dendrite maturation in adult hippocampal neurogenesis is independent of the regulation of precursor cell proliferation. *BMC Neurosci* 7:77.
- Prohovnik I, Arnold SE, Smith G, Lucas LR (1997) Physostigmine reversal of scopolamine-induced hypofrontality. *J Cereb Blood Flow Metab* 17:220-228.
- Ramirez-Rodriguez G, Ortiz-Lopez L, Dominguez-Alonso A, Benitez-King GA, Kempermann G (2011) Chronic treatment with melatonin stimulates dendrite maturation and complexity in adult hippocampal neurogenesis of mice. *J Pineal Res* 50:29-37.
- Schmued LC, Hopkins KJ (2000) Fluoro-Jade B: a high affinity fluorescent marker for the localization of neuronal degeneration. *Brain Res* 874:123-130.
- Shi J, Liu Q, Wang Y, Luo G (2010) Coadministration of huperzine A and ligustrazine phosphate effectively reverses scopolamine-induced amnesia in rats. *Pharmacol Biochem Behav* 96:449-453.
- Tanapat P, Hastings NB, Reeves AJ, Gould E (1999) Estrogen stimulates a transient increase in the number of new neurons in the dentate gyrus of the adult female rat. *J Neurosci* 19:5792-5801.
- Tota S, Nath C, Najmi AK, Shukla R, Hanif K (2012a) Inhibition of central angiotensin converting enzyme ameliorates scopolamine induced memory impairment in mice: role of cholinergic neurotransmission, cerebral blood flow and brain energy metabolism. *Behav Brain Res* 232:66-76.
- Tota S, Hanif K, Kamat PK, Najmi AK, Nath C (2012b) Role of central angiotensin receptors in scopolamine-induced impairment in memory, cerebral blood flow, and cholinergic function. *Psychopharmacology* 222:185-202.
- Velazquez R, Ash JA, Powers BE, Kelley CM, Strawderman M, Luscher ZI, Ginsberg SD, Mufson EJ, Strupp BJ (2013) Maternal choline supplementation improves spatial learning and adult hippocampal neurogenesis in the Ts65Dn mouse model of Down syndrome. *Neurobiol Dis* 58:92-101.
- Wang X, Wang ZH, Wu YY, Tang H, Tan L, Gao XY, Xiong YS, Liu D, Wang JZ, Zhu LQ (2013) Melatonin attenuates scopolamine-induced memory/synaptic disorder by rescuing EPACs/miR-124/Egr1 pathway. *Mol Neurobiol* 47:373-381.
- Yan BC, Park JH, Kim IH, Shin BN, Ahn JH, Yoo KY, Lee DS, Kim MJ, Kang IJ, Won MH (2012) Chronological changes in inflammatory cytokines immunoreactivities in the mouse hippocampus after systemic administration of high dosage of tetanus toxin. *Exp Brain Res* 223:271-280.
- Yoo DY, Kim W, Yoo KY, Lee CH, Choi JH, Kang IJ, Yoon YS, Kim DW, Won MH, Hwang IK (2011a) Effects of *Nelumbo nucifera* rhizome extract on cell proliferation and neuroblast differentiation in the hippocampal dentate gyrus in a scopolamine-induced amnesia animal model. *Phytother Res* 25:809-815.
- Yoo DY, Woo YJ, Kim W, Nam SM, Lee BH, Yeun GH, Yoon YS, Won MH, Park JH, Hwang IK (2011b) Effects of a new synthetic butyrylcholinesterase inhibitor, HBU-39, on cell proliferation and neuroblast differentiation in the hippocampal dentate gyrus in a scopolamine-induced amnesia animal model. *Neurochem Int* 59:722-728.
- Yoo DY, Shin BN, Kim IH, Kim DW, Yoo KY, Kim W, Lee CH, Choi JH, Yoon YS, Choi SY, Won MH, Hwang IK (2012) Effects of sensitive to apoptosis gene protein on cell proliferation, neuroblast differentiation, and oxidative stress in the mouse dentate gyrus. *Neurochem Res* 37:495-502.
- Yu DK, Yoo KY, Shin BN, Kim IH, Park JH, Lee CH, Choi JH, Cho YJ, Kang IJ, Kim YM, Won MH (2012) Neuronal damage in hippocampal subregions induced by various durations of transient cerebral ischemia in gerbils using Fluoro-Jade B histofluorescence. *Brain Res* 1437:50-57.
- Zhang E, Shen J, So KF (2014) Chinese traditional medicine and adult neurogenesis in the hippocampus. *J Tradit Complement Med* 4:77-81.
- Zhang J, Groff RE, Dayawansa S (2013) Imipramine treatment increases cell proliferation following fluid percussion brain injury in rats. *Neurol Res* 35:247-254.

Copypedited by Jackson C, Li CH, Song LP, Liu WJ, Zhao M